Fuel Processing Technology 90 (2009) 1175–1182

Contents lists available at ScienceDirect

Fuel Processing Technology

journal homepage: www.elsevier.com/locate/fuproc

# Biodiesel compatibility with carbon steel and HDPE parts

Marcia Marie Maru [a,*], Marcia Maria Lucchese [a], Cristiano Legnani [a], Welber Gianini Quirino [a], Andrea Balbo [a], Isabele Bulhões Aranha [a], Lílian Terezinha Costa [a], Cecília Vilani [a], Lídia Ágata de Sena [a], Jailton Carreteiro Damasceno [a], Talita dos Santos Cruz [a], Leandro Reis Lidízio [a], Rui Ferreira e Silva [b], Ado Jorio [a,d], Carlos Alberto Achete [a,c]

[a] Divisão de Metrologia de Materiais-DIMAT, Inmetro, Av. Nossa Senhora das Graças 50, CEP 25250-020, Duque de Caixas, RJ, Brazil
[b] Ceramics Eng. Dept., CICECO, University of Aveiro, 3810-193 Aveiro, Portugal
[c] Programa de Engenharia Metalúrgica e de Materiais-PEMM, Centro de Tecnologia, Bloco F, Cidade Universitária, Universidade Federal do Rio de Janeiro-UFRJ, CEP 21949-900, Rio de Janeiro, RJ, Brazil
[d] Departamento de Física, Universidade Federal de Minas Gerais, Av. Antônio Carlos 6627, CEP 30123-970, Pampulha, Belo Horizonte, MG, Brazil

ARTICLE INFO

*Article history:*
Received 5 October 2008
Received in revised form 3 May 2009
Accepted 12 May 2009

*Keywords:*
Biodiesel
Compatibility
Immersion
Carbon steel
HDPE

ABSTRACT

Compatibility of the new environmentally-friendly alternative of diesel engine fuels, biodiesel, with storage and engine part materials, is still an open issue. In this work, the interaction between three fuels (petroleum diesel and two types of biodiesel — soybean and sunflower) and two materials (carbon steel and high density polyethylene) used in storage and automotive tanks, is analyzed in detail. A wide set of characterization techniques was used to evaluate the changes in both solid and fluid materials, as weight change measurement, optical, scanning electron and atomic force (AFM) microscopies, Raman and FTIR spectroscopies, and differential scanning calorimetry. The AFM technique allowed detecting surface roughness and morphology changes in the metallic material following the trends in the weight losses. In the case of polymeric material, weight gain by fluid absorption occurred, being detected by the spectroscopic techniques. The biodiesel fuels underwent some ageing however this phenomenon did not affect the interaction between the biodiesel fuels and the substrates. The petrodiesel, which did not age, caused more significant degradation of the substrates.



## 1. Introduction

Currently, biodiesel is extensively studied as a substitute of fossil fuels used in compression ignition engines due to its beneficial features concerning economical, environmental and energy issues. A still open issue is its compatibility with different materials. Biodiesels become unstable when they exhibit a net increase in insoluble formation, acid number and viscosity. The time to reach unacceptable levels of such features varies with the biodiesel sample but some of them become "old" fuels after 4–8 weeks of storage, when they lead to aggressive peroxides that may oxidize storage tanks, pipes and pressure vessels, and the diesel engine parts [1]. Moreover, biodiesels can be often produced out-of-specification, thus becoming contaminated with corrosive agents as water and sulfur [2]. The addition of inhibitors extends the time before corrosion starts in metallic parts [3].

Only few works can be found in the literature with detailed studies on the materials surface change after prolonged contact with biodiesels [4–6]. Kaul et al. [4] have studied the interaction between different types of biodiesel and metal parts of a diesel engine (aluminum piston and ferrous alloy liner). The non-ferrous metal did not experience any change due to contact with the fuels except when a high-sulfur content biodiesel was used. On the other hand, the ferrous piston liner presented measurable weight loss with all fuels, especially when in contact with the most aggressive biodiesel.

A study on poultry derived biofuels, including corrosion analysis on other metals (carbon steel, admiralty brass, copper, grey cast iron and 316 stainless steel), revealed that copper and brass were highly affected by the fuel, suffering from marked weight loss by a pitting mechanism and extensive surface covering by deposits [5]. Here, the carbon steel and the stainless steel showed no weight loss or visible corrosion. Random pitting was observed in the grey cast iron.

A recent study sponsored by the Steel Tank Institute on the corrosion rate of steel in various biodiesels and biodiesel/petroleum diesel blends using electrochemical impedance spectroscopy, concluded that both the biodiesel and the blends caused insignificant level of corrosion [6]. However, a small amount of surface rusting was observed due to reaction between the surface oxide layer of the metal and the fuel blend [6]. Biodiesel is a better solvent than petroleum diesel capable of dissolving any deposited layers of foreign material on the steel surface, which can be critical in some systems, like injection

* Corresponding author. Av. Nossa Senhora das Graças 50 CEP 25250-020 Duque de Caixas, RJ, Brazil. Tel.: +55 21 2679 9721; fax: +55 21 2679 9021.
*E-mail address:* mmmaru@gmail.com (M.M. Maru).

0378-3820/$ – see front matter 
doi:10.1016/j.fuproc.2009.05.014

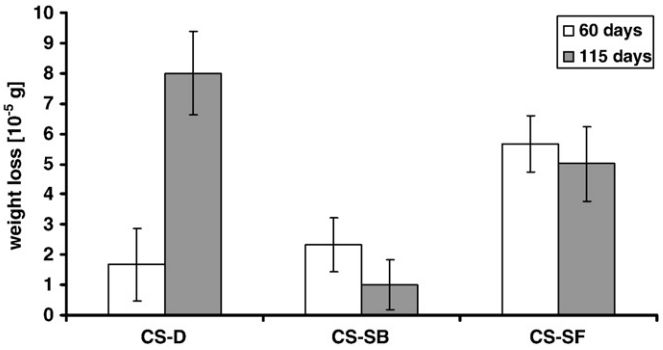


**Fig. 1.** Weight loss of CS samples after immersion tests. CS-D: in petroleum diesel; CS-SB: in soybean biodiesel; CS-SF: in sunflower biodiesel.

pumps, due to clogging of filters. Another issue is that biodiesel is electrically more conductive than gasoline and petrodiesel fuel and thus it may induce galvanic metal corrosion mechanism in steels [7].

Regarding the compatibility with polymers, most of the work has been published reporting on the swelling phenomenon and degradation in the mechanical properties of elastomeric parts as sealants [8,9]. Swelling is related to an increase in volume of the material due to its interaction with a solvent material that is not able to solubilize it, being the solvent retained into the material. Such phenomenon is established when there is some chemical affinity between the solute and the solvent materials, in this case the polymer and the biofuel.

Considering other types of polymeric materials, namely polyethylene that is used in automotive tanks, no published papers could be found on the compatibility between biofuels and this type of polymer. However, it is mentioned in some websites that biodiesel materials are not compatible with this type of polymer [10,11].

The present work aims to analyze the interaction between three fuels (petroleum diesel and two types of biodiesel) and two materials (carbon steel and high density polyethylene). Carbon steel (CS) and high density polyethylene (HDPE) are common materials that are often in contact with biodiesels, for example, as large storage tanks in the former case and automotive tanks in the later. Soybean and sunflower derived biodiesels, typical types produced from vegetable oils, were tested in this investigation. In contrast with the published works on static immersion tests, where only optical microscopy and weight loss evaluation was used to evaluate the changes in the materials, a wide set of characterization techniques is used here: weight loss, optical, scanning electron and atomic force microscopies, Raman and Fourier Transform Infrared (FTIR) spectroscopies, and differential scanning calorimetry (DSC).

## 2. Experimental

The tested fluids were: a commercial petroleum diesel (containing 870 ppm total sulfur, coded as D), a soybean derived biodiesel (coded as SB) and a sunflower derived biodiesel (coded as SF). The fluids were analyzed in terms of thermal behavior by Differential Scanning Calorimeter (TA Instruments DSC Q1000), using aluminium hermetic pan in order to prevent evaporation during the tests. The fluids were first cooled to −90 °C, at 10 °C/min and then were heated to 20 °C at 0.5 °C/min, in order to detect all thermal events and differentiate their thermal behaviours. Raman measurements (Horiba Jobin-Yvon T64000) were carried out on the fluids at room temperature. The samples were focused with a 50× objective in a microscope attached to the spectrometer, being excited by argon laser line at 514 nm with 20 mW of power. No laser induced heating occurs as evidenced by comparative tests reducing the laser power and rotating samples. The spectra were acquired in 5 integrations of 10 s and calibrated for frequency using the Raman spectra of silicon. Fourier Transform Infrared (FTIR) analysis (PerkinElmer

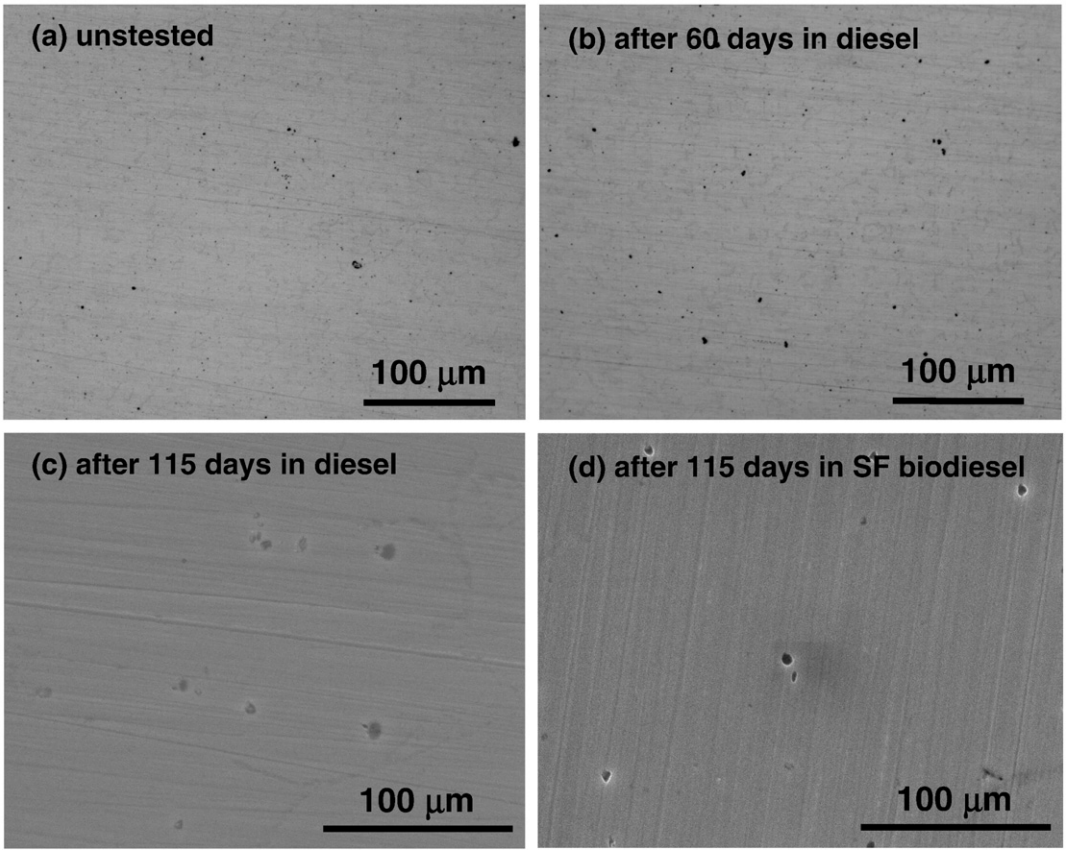


**Fig. 2.** Optical (a,b) and scanning electron (c,d) micrographs of CS surfaces. (a) Untested; (b) after 60 days in diesel; (c) after 115 days in diesel; (d) after 115 days in SF biodiesel.

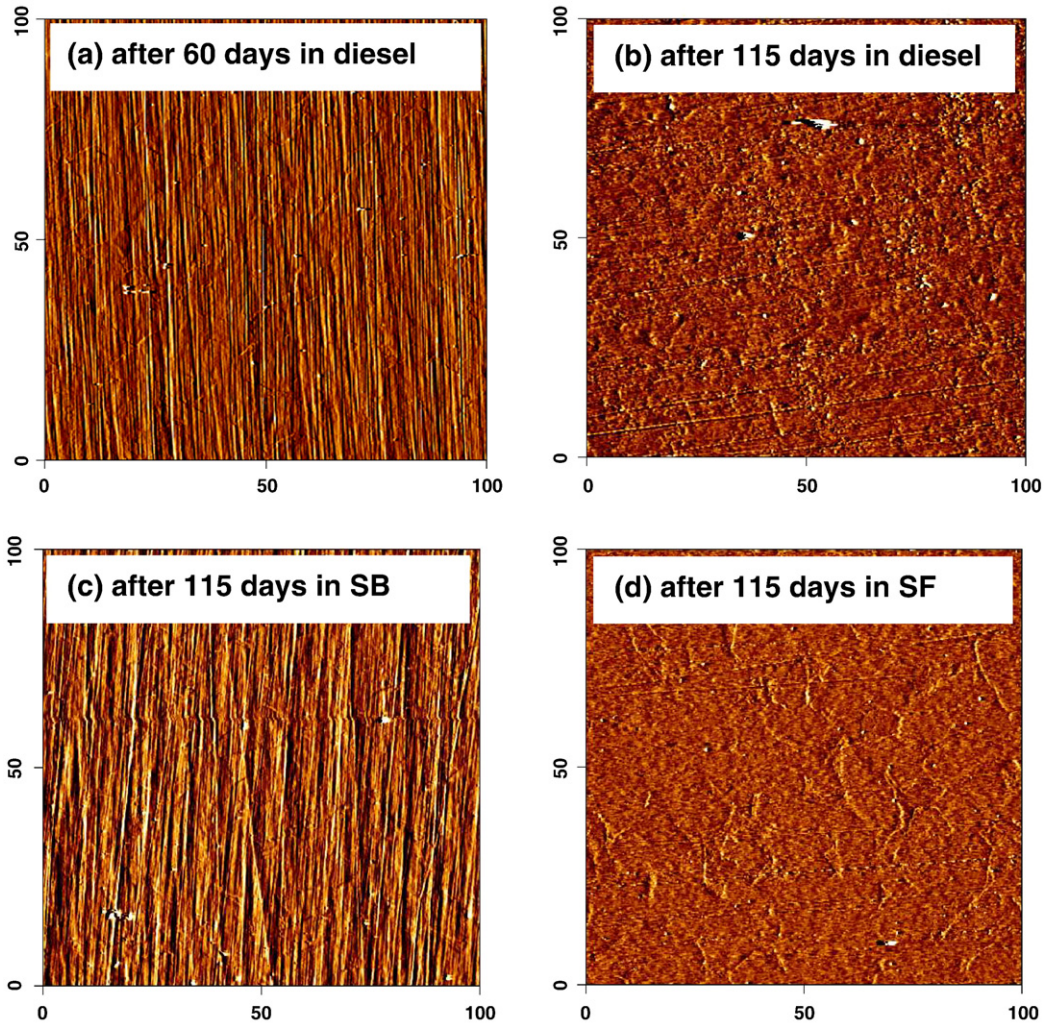


**Fig. 3.** Images of CS surfaces after immersion tests measured by atomic force microscope (scale in micrometers). (a) 60 days in diesel; (b) 115 days in diesel; (c) 115 days in SB biodiesel; (d) 115 days in SF biodiesel.

Spectrum GX FTIR system) was performed using a Horizontal Attenuated Total Reflectance (HATR) cell, covering the 650–4000 $cm^{-1}$ spectral range. Each FTIR-HATR spectrum was the average of 30 scans, using air as reference, at 4 $cm^{-1}$ of nominal spectra resolution.

The tested solid materials were structural carbon steel (ASTM A36, coded as CS) and high density polyethylene (coded as HDPE). The materials were received as sheets of 4 mm (metal) and 3 mm (polymer) in thickness; test samples were obtained by cutting the sheets to 10 mm × 10 mm (metal) and 20 mm × 20 mm (polymer) squares. The metallic samples were surface finished by paper grinding until 1200 mesh followed by unidirectional polishing with 9 μm and 3 μm diamond paste. Cleaning of metal samples was done in ultrasonic bath with ethanol, washing with acetone and drying in air flow, accordingly to ASTM E3 standard [12]. Polymer samples in the as-received condition were cleaned in ultrasonic bath with liquid detergent diluted in distilled water, washed with distilled water and dried in air flow.

The static immersion tests were carried out with the samples placed at the bottom of amber colored bottles containing 20 ml of fluid, under a constant temperature of 60 °C. Examinations on the fluids and solid parts were carried out after 60 and 115 days for the tests with metal and 75 and 125 days for the tests with polymer. After immersion, the metallic parts were analyzed in detail by several techniques: weight loss evaluation using a scale with $10^{-5}$ g of accuracy (Metler Toledo XS205), and surface observation by optical microscopy (Olympus BX51M), scanning electron microscopy (FEI Quanta 200) and atomic force microscopy (JPK Instruments NanoWizard). The atomic force microscopy was used to estimate the Rq (root mean square) surface roughness parameter.

The error bars of mass measurements correspond to the combined uncertainty [13], considering the repeatability of measurements of mass, before (3 measurements) and after (6 measurements) the immersion tests. The error bars of roughness measurements correspond to the

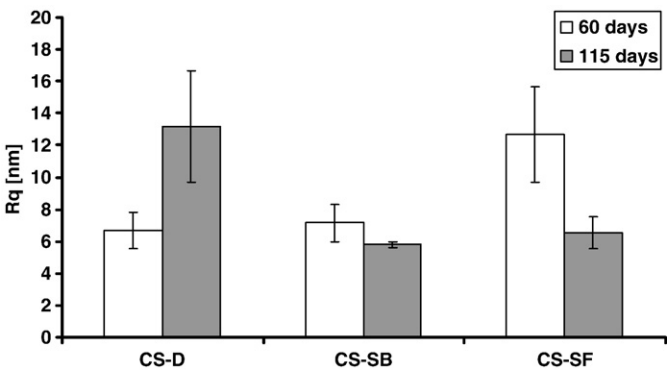


**Fig. 4.** Rq (root mean square) roughness parameter of CS samples after immersion tests. CS-D: in petroleum diesel; CS-SB: in soybean biodiesel; CS-SF: in sunflower biodiesel.

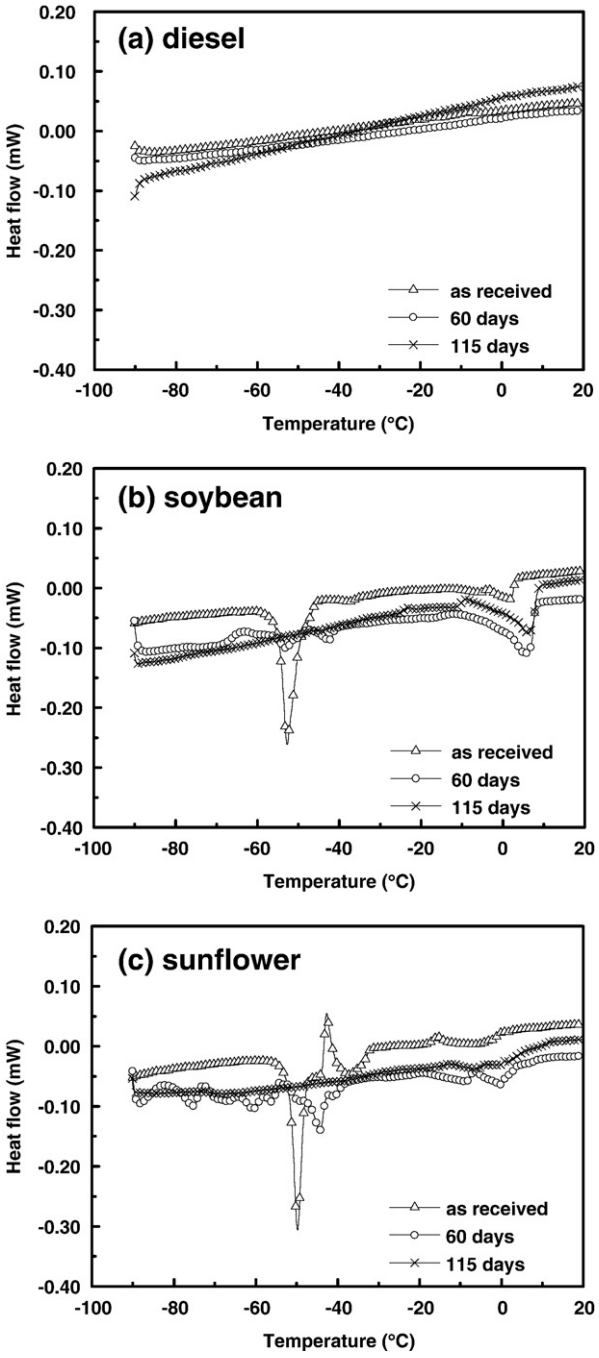


**Fig. 5.** DSC analyses of fluids before and after immersion tests. (a) Diesel; (b) Soybean; (c) Sunflower.

standard uncertainty [13], which was estimated considering the repeatability of 3 measurements.

Raman spectra of the HDPE polymer were acquired in the same conditions as described for the fluids but with 2 integrations of 80 s. Polymer samples were also analyzed by FTIR spectroscopy in the same condition of fluids, in a plane HATR cell.

## 3. Results and discussion

### 3.1. Carbon steel

Fig. 1 shows the complete set of weight loss data after 60 and 115 days of immersion of carbon steel in soybean biodiesel (CS-SB), sunflower biodiesel (CS-SF) and petroleum diesel (CS-D) fuels. It can be observed that time is relevant in the diesel fuel action on the CS sample as the metal experiences a fourfold weight loss between the two time periods. Conversely, the weight of the samples exposed to biodiesel did not change after 60 days. It was found that soybean biodiesel was more compatible with carbon steel than petroleum diesel and sunflower biodiesel.

Optical and SEM microscopies were used to analyze the surface morphology. Representative micrographs are presented in Fig. 2 for surfaces before and after immersion. Optical microscopy did not show any sign of surface etching with respect to the untested surface. This is evidenced by comparing Fig. 2b (after 60 days in petroleum diesel) with Fig. 2a (untested). In addition, SEM microscopy of the samples with the highest weight losses (CS-D and CS-SF gray columns in Fig. 1) could not reveal any type of etching, as evidenced in Fig. 2c (after 115 days in petroleum diesel) and Fig. 2d (after 115 days in sunflower biodiesel).

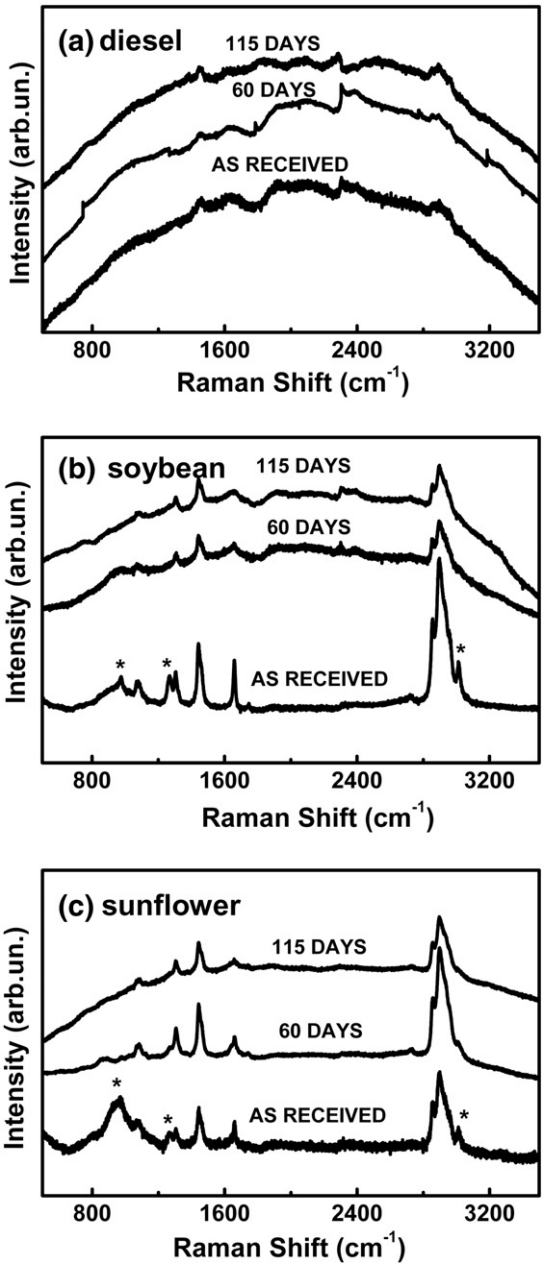


**Fig. 6.** Raman spectra (stacked baseline) of fluids before and after immersion tests. (a) Diesel; (b) Soybean; (c) Sunflower. Stars in panel c refer to the peaks corresponding to =C–H bonds, still present in the spectrum of sunflower biodiesel after immersion test.

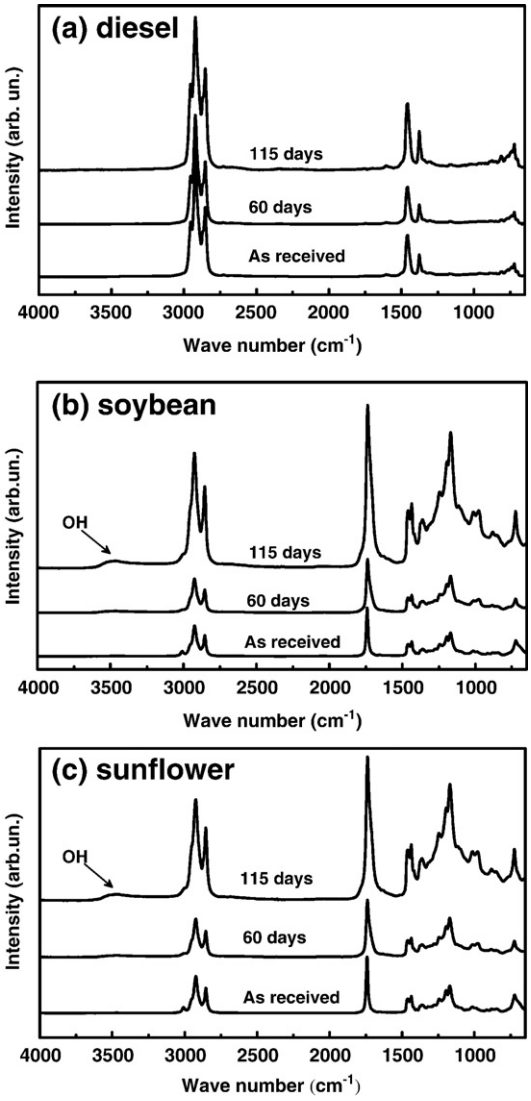


**Fig. 7.** FT-IR spectra of fluids before and after immersion tests. (a) Diesel; (b) Soybean; (c) Sunflower.

In order to highlight any morphological features that could indicate the action of the fluids on the CS samples, atomic force microscopy (AFM) was employed. Fig. 3 gives typical aspects of nearly unmodified (Fig. 3a and c) and modified (Fig. 3b and d) surfaces. Fig. 3a shows the surface of the CS sample after 60 days of immersion in petroleum diesel. This surface is that of inexpressive weight loss (Fig. 1, CS-D white column). In this case, the unidirectional grooves caused by surface preparation step are still very noticeable. The same appearance is seen in the CS sample after 115 days in soybean biodiesel (Fig. 3c), which also showed no relevant weight change within this time period (Fig. 1, CS-SB gray column). On the other hand, the typical grooved morphology of as-prepared surfaces was modified in the case of the samples that underwent significant weight losses after 115 days of immersion (CS-D and CS-SF gray columns in Fig. 1). In this case, a more isotropic surface morphology is observed (Fig. 3b for CS-D sample and Fig. 3d for CS-SF sample), resulting from a uniform etching throughout the entire surface. The corresponding root mean square surface roughness (Rq) measurements are plotted in Fig. 4. It is important to note that a correlation exists between this graph and the weight loss plot in Fig. 1. The most visible trends in Fig. 1, i.e. the influence of time regarding the diesel and the compatibility of soybean biodiesel, are pointed out by both methods of analysis.

The presented results concerning the action of different fuels on carbon steel show that this ferrous alloy undergoes a certain level of etching. Several techniques were used to accomplish this observation which allowed a different assessment from that of literature [5] where carbon steel is described to have no weight loss after immersion testing in biodiesel. Similarly to Kaul et al. [4], distinct varieties of biodiesel produced dissimilar effects in ferrous alloys, the sunflower biodiesel being the most aggressive one in the present work. The reason for this different behavior can be related to the differences in the chemical components of these feedstocks. It can lead to particular degradation processes, generating products with distinct degree of corrosivity.

DSC analysis, Raman and FT-IR spectroscopies were performed in the collected fluid samples in order to investigate a possible degradation of the biodiesels during the testing time periods and possible differences in the chemical structure among the fluids.

Fig. 5 shows the results of the DSC analysis performed in the temperature range from −90 to 20 °C for the three tested fuels. The diesel fuel did not experience any phase transformation within this temperature range, either prior or after the immersion test (Fig. 5a). Concerning the analyses of the biodiesel fuels in the as-received condition, endothermic and exothermic peaks are noticed, which should correspond to melting and crystallization of components, specific of each biofuel material (Fig. 5b for SB biodiesel and c for SF biodiesel). The thermal behavior of both biodiesels changed after 60 days of immersion, since the main peaks disappeared in these curves. Some hypotheses can be stated to explain the change in the thermal behavior during the immersion test, such as the evaporation of volatile components of the biodiesel material and the change in the chemical structure due to a degradation process. More studies on biodiesel stability are under way.

The relevant Raman spectra of the different fuels are shown in Fig. 6. The diesel spectrum in Fig. 6a exhibits a broad emission characteristic of photoluminescence. In this case the Raman features are not visible. For the soybean biodiesel (Fig. 6b), peaks at 960 $cm^{-1}$ and 1267 $cm^{-1}$, corresponding to out of plane symmetric bending modes of unconjugated =C–H bonds [14,15] disappeared after 60 and 115 days, along with the peak at 3313 $cm^{-1}$ assigned to the asymmetric stretching mode of the same system [14]. A similar behavior is observed for the sunflower biofuel (Fig. 6c) after 115 days, but after 60 days, those peaks are still present, although with a very low intensity (see insets in Fig. 6c; stars refer to the peaks corresponding to =C–H bonds, still present in the spectrum of sunflower biodiesel after immersion test). This behavior indicates that the sunflower biodiesel experienced a slightly less ageing than the soybean variety.

The FT-IR spectra shown in Fig. 7 revealed a broadening of the C=O peak at ~1740 $cm^{-1}$ [15] and the appearance of hydroxyl group at ~3500 $cm^{-1}$ [16], in both the biodiesel fuels after 115 days of immersion. Both features are thought to be related to secondary degradation products of decomposition process promoted by factors

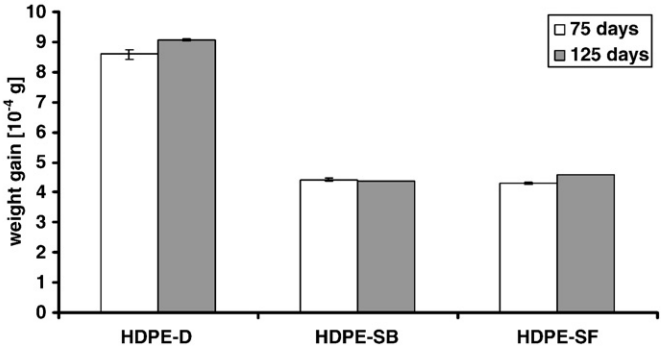


**Fig. 8.** Weight gain of HDPE samples after immersion tests. HDPE-D: in petroleum diesel; HDPE-SB: in soybean biodiesel; HDPE-SF: in sunflower biodiesel.

such as temperature and presence of metals. These secondary degradation products are formed in different amounts and their chemistry depends on the unsaturated fatty acid content in the biodiesel [17,18]. Broadening of the C=O peak at ~1740 $cm^{-1}$ can be assigned to aldehyde carbonyl and ester carbonyl groups that are mutually overlapped.

All the techniques employed to analyze the fluids have indicated that biodiesels experienced some ageing, contrarily to petrodiesel. This is in agreement with the literature, where it is reported that biodiesels are far more prone to oxidation than petrodiesels [1,19]. However, this phenomenon did not affect the carbon steel, as biodiesel caused a smaller material modification compared to diesel. Such different behavior of petroleum diesel and biodiesel cannot be attributed to differences in electrical conductivity since if they were determinant, galvanic corrosion would happen preferably with the steel/biodiesel pair [6]. The higher degradation of the metal surface when in contact with petrodiesel is probably related to its sulfur content. Hydrocarbons themselves do not cause corrosion, but the acidic compounds, the sulfur molecules or presence of water in the diesel fuel can cause chemical attack [20]. A probable mechanism is iron sulphide formation from reaction with sulphur compounds present in petrodiesel, such as mercaptans and thiophenes [21].

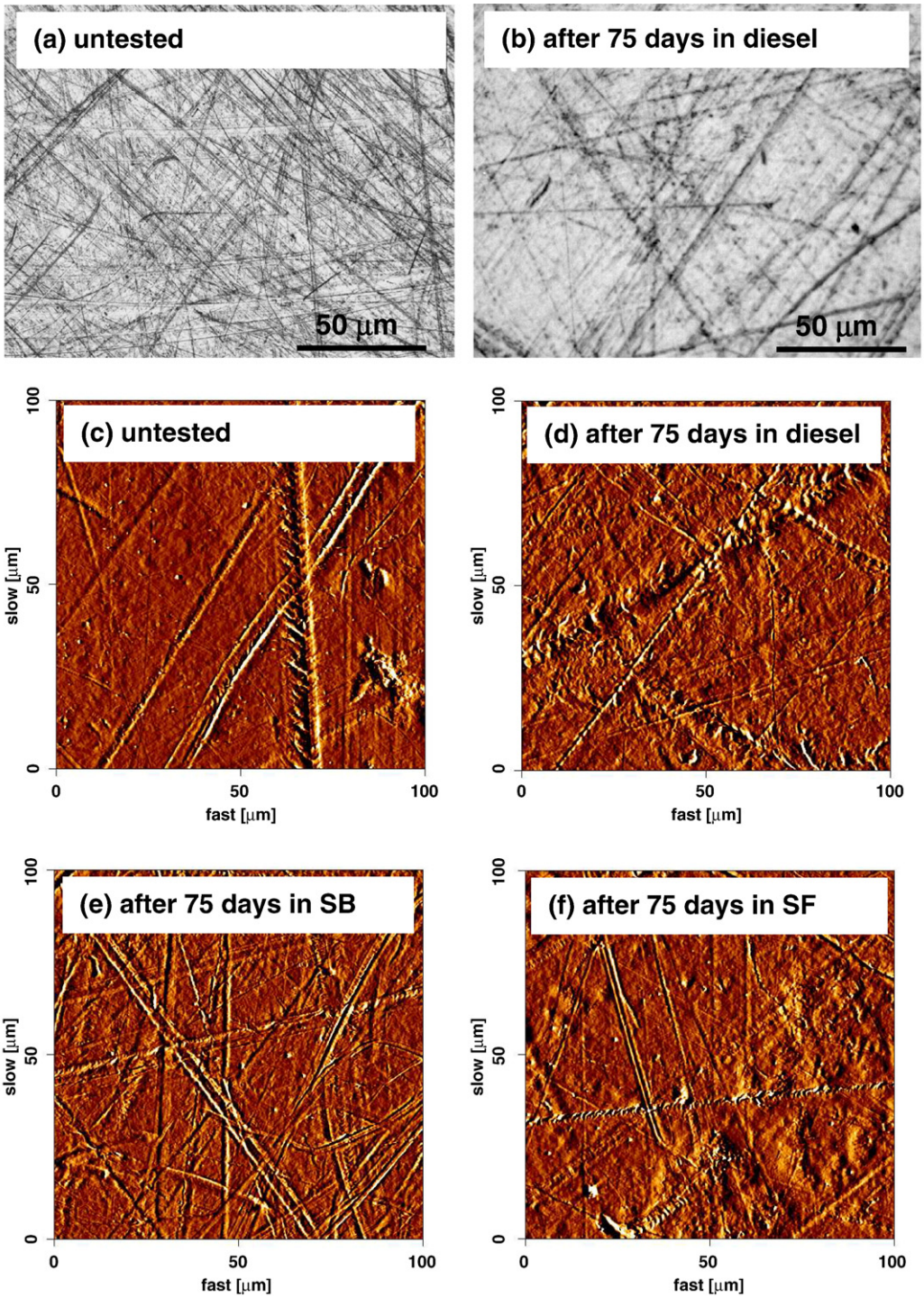


**Fig. 9.** Images of HDPE surfaces measured by optical (a and b) and atomic force microscope (c, d, e and f). (a) Untested; (b) after 75 days in diesel; (c) untested; (d) after 75 days in diesel; (e) after 75 days in SB biodiesel; (f) after 75 days in SF biodiesel.

### 3.2. High density polyethylene

The immersion experiments carried out with the HDPE polymer followed a similar protocol as that of carbon steel. The weight change as a function of exposure time and fuel type is shown in Fig. 8. Interestingly, instead of loosing mass, the polymer experienced significant weight gain. Similarly to the carbon steel exposures, petrodiesel caused larger weight change than the biodiesels. In this case, the two biodiesel varieties caused the same effect on the polymer. Visual inspection (not presented here) revealed a yellowish appearance of HDPE samples after being immersed in all fuels, compared to the white color of the pristine samples. Both information, weight gain and discoloration, suggest a fluid absorption phenomenon, which can be interpreted as swelling occurrence, that is commonly reported for polymers, especially elastomers [8,9]. It is worth noting that the swelling occurs during the first 75 days of immersion and remains stable, with no further fluid absorption.

Fig. 9 shows the main morphological characteristics of the HDPE samples. The optical micrographs (Fig. 9a — untested and Fig. 9b — after 75 days in petroleum diesel) reveal that the tested surfaces are identical to the unexposed ones. When observed by AFM, the surfaces of the samples tested with all the three fluids (Fig. 9d to f) seemed to experience some slight change in the surface morphology mainly in the flat areas, compared to the unexposed one (Fig. 9c), but the change in terms of Rq did not provide clear trends, which can be attributed to the high roughness of HDPE surface itself.

Raman and FT-IR spectroscopy analyses on the HDPE surfaces were also performed. The Raman spectra in Fig. 10a reveal that the chemistry of the polymer immersed in both the petrodiesel and biodiesel fuels did not change after 75 days of exposure. In case of the petrodiesel, the HDPE peaks are somewhat masked by photoluminescence (see Fig. 6a). The FT-IR spectra in Fig. 10b show the appearance of a biodiesel peak (see the main peak around 1740 $cm^{-1}$ in Fig. 7b and c, assigned as C=O) on the polymer surface. In the case of diesel, its main FT-IR peak occurs at ~2920 $cm^{-1}$ (see Fig. 7a), which is masked by the polymer peaks in Fig. 10b. The Raman and FT-IR spectroscopies, as well as DSC analysis, were also performed on the fluid samples collected after immersion. The results were similar to those found in case of carbon steel, that is, the biofuel fluids in contact with HDPE showed signs of ageing during the immersion tests.

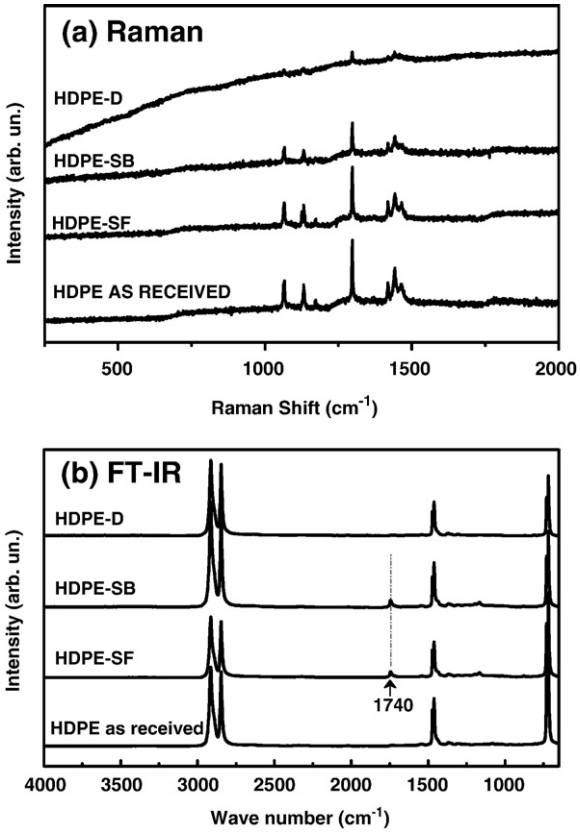


**Fig. 10.** Spectroscopic analyses of HDPE before and after immersion in fuels for 75 days. (a) Raman spectra; (b) FT-IR spectra.

## 4. Conclusions

The action of petroleum diesel, soybean and sunflower biodiesel on carbon steel causes a low level of surface etching, as demonstrated by several characterization techniques. The weight loss after 115 days experienced by the metal immersed in petrodiesel is small, in the range of $10^{-5}$ g, but slightly higher than that in case of the biodiesel varieties. Moreover, the soybean biodiesel proved to be less reactive to the metal than the sunflower biofuel. AFM was the only microscopy technique that allowed distinguishing the different levels of surface etching on carbon steel. It is worth noting that the trend in the surface roughness values obtained from AFM measurements correlates well with that of the weight loss values. The present finding does not agree with the general statement that biodiesel is inert to carbon steel.

In the case of the HDPE polymers, the interaction with the different fuels is much more prominent. The polymer undergoes a net weight gain, one order of magnitude higher, in absolute values, than the weight loss of the carbon steel material. The use of Raman and FT-IR spectroscopies confirmed that the tested fuels were absorbed by the polymer. However, this weight gain is still very small, in the order of $10^{-4}$ g, and remains stable after 75 days of exposure. The petroleum diesel was again found to cause higher weight gain, that is, swelling, than the biodiesels. Microscopy techniques did not show significant differences in the HDPE surface morphology after immersion in the fuel media.

The analyses performed in the tested fluids showed that ageing took place only in biodiesels, but this phenomenon did not cause degradation or corrosion of carbon steel or HDPE, since petroleum diesel did not age but exerted the most significant material degradation.

## Acknowledgement

The authors acknowledge Dr. Romeu Daroda from Inmetro for supplying the fuel and the material samples and for helpful discussion, and financial support from Finep, CNPq and Faperj. R.F. Silva acknowledges EuropeAid/120707/C/SER/Br n.PAIIPME-ATI-POA2-022 project.

## References

[1] R.L. McCormick, M. Ratcliff, L. Moens, R. Lawrence, Several factors affecting the stability of biodiesel in standard accelerated tests, Fuel Process. Technol. 88 (2007) 651–657.
[2] Y.C. Sharma, B. Singh, S.N. Upadhyay, Advancements in development and characterization of biodiesel: a review, Fuel 87 (2008) 2355–2373.
[3] B. Miksic, M. Kharshan, A. Furman, B. Wuertz, I. Rogan, Biodegradable VPCI building block for biofuels, Goriva Maziva 46-5 (2007) 403–418.
[4] S. Kaul, R.C. Saxena, A. Kumar, M.S. Negi, A.K. Bhatnagar, H.B. Goyal, A.K. Gupta, Corrosion behavior of biodiesel from seed oils of Indian origin on diesel engine parts, Fuel Process. Technol. 88 (2007) 303–307.
[5] D.P. Geller, T.T. Adams, J.W. Goodrum, J. Pendergrass, Storage stability of poultry fat and diesel fuel mixtures: specific gravity and viscosity, Fuel 87 (2008) 92–102.
[6] M.A. Jakab, S.R. Westbrook, S.A. Hutzler, A final report for testing for compatibility of steel with biodiesel. SwRI Project No. 08.13070, Steel Tank Institute, Southwest Research Institute, TX, USA (2008) 16p. www.biodiesel.org/resources/reportsdatabase/reports/gen/20080407_gen385.pdf [accessed 02/09/2008].
[7] L.E. Gonzalez Prieto, P.A. Sorichetti, S.D. Romano, Electric properties of biodiesel in the range from 20 Hz to 20 MHz. Comparison with diesel fossil fuel, Int. J. Hydrogen Energy 33 (2008) 3531–3537.
[8] W. Trakarnpruk, S. Porntangjitlikit, Palm oil biodiesel synthesized with potassium loaded calcined hydrotalcite and effect of biodiesel blend on elastomer properties, Renew. Energy 33 (2008) 1558–1563.

[9] B. Flitney, Which elastomer seal materials are suitable for use in biofuels? Seal. Technol. (2007) 8–11.
[10] M. Zappi, R. Hernandez, D. Sparks, J. Horne, M. Brough, A Review of the Engineering Aspects of the Biodiesel Industry, MSU E-TECH Laboratory Report ET-03-003, Mississippi University Consortium for the Utilization of Biomass (2003) p.12. http://www.southeastdiesel.org/Photos/Library/Ag/Eng_AspectsCh1.pdf [accessed in September 2008].
[11] Biodiesel handling and use guidelines. Report DOE/GO-102006-2358 Third Edition September 2006. US Department of Energy, p. 16. http://www.nrel.gov/vehiclesandfuels/npbf/pdfs/40555.pdf [accessed in September 2008].
[12] An American National Standard. Standard Practice for Preparation of Metallographic Specimens, ASTM E3 (1995).
[13] Guide to the expression of uncertainty in measurement (GUM), ISO/IEC Guide 98 (1995).
[14] Espectrometria no Infravermelho, in: R.M. Silverstein, F.X. Webster (Eds.), Identificação Espectrométrica de Compostos Orgânicos, sixth ed., LTC, Rio de Janeiro, Brazil, 2000.
[15] R.C. Barthus, R.J. Poppi, Determination of the total unsaturation in vegetable oils by Fourier transform Raman spectroscopy and multivariate calibration, Vib. Spectrosc. 26 (2001) 99–195.
[16] J. Socrates, Infrared and Raman Characteristic Group Frequencies, Third ed.John Wiley & Sons LTDA, England, 2001.
[17] O. Herbinet, W.J. Pitz, C.K. Westbrook, Detailed chemical kinetic oxidation mechanism for a biodiesel surrogate, Combust. Flame 154 (2008) 507–528.
[18] G. Knothe, Some aspects of biodiesel oxidative stability, Fuel Process. Technol. 88 (2007) 669–677.
[19] D. Bajpai, D.k. Tyagi, Biodiesel: source, production, composition, properties and its benefits, J. Oleo Sci. 55-10 (2006) 478–502.
[20] J. Hancsok, M. Bubálik, A. Beck, J. Baladincz, Development of multifunctional additives based on vegetable oils for high quality diesel and biodiesel, Chem. Eng. Res. Design (2008) 793–799 8 6.
[21] D.J. Pack, 'Elemental Sulphur' formation in natural gas transmission pipelines, PhD Thesis, The University of Western Australia, 2005. Available in: http://theses.library.uwa.edu.au/adt-WU2005.0096/public/02whole.pdf (2009 March).